

# Three-dimensional magneto-resistive random access memory devices based on resonant spin-polarized alternating currents

Christoph Vogler,<sup>a)</sup> Florian Bruckner, Markus Fuger, Bernhard Bergmair, Thomas Huber, Josef Fidler, and Dieter Suess

Vienna University of Technology, Institute Solid State Physics, Vienna, 1040 Austria

(Received 4 April 2011; accepted 5 May 2011; published online 16 June 2011)

Selective switching of a magneto-resistive random access memory (MRAM) multilayer stack is demonstrated using resonant spin-polarized alternating currents (AC) superimposed on spin-polarized direct currents. Finite element micromagnetic simulations show that the use of frequency triggered AC allows one to maximize the transferred spin transfer torque selectively in order to merely reverse the magnetization of a single storage layer in a stack. Using layers with different resonance frequencies, which are realized by altering the anisotropy constants, allows one to address them by tuning the AC frequency. A rapid increase of the storage density of MRAM devices is shown by using three-dimensional sandwich structures. © 2011 American Institute of Physics. [doi:10.1063/1.3596813]

## I. INTRODUCTION

Spin-polarized currents exert a torque, called spin transfer torque (STT), on the magnetization of a device. Recently MRAM based on STT has become one promising candidate for a non-volatile “Universal Memory”.<sup>1</sup> The basic concept relies on the prediction of Berger and Slonczewski. In their pioneering works on ferromagnet/insulator/ferromagnet systems<sup>2</sup> and on layered systems with a metallic spacer<sup>3,4</sup> Berger and Slonczewski have considered the emission of spin-polarized electric currents from one magnetic layer to another. As a consequence the effect of current induced magnetic switching was observed for example in Refs. 5–7 and Ref. 8. Very recently, it was experimentally demonstrated that the application of spin-polarized AC can assist the reversal.<sup>9,10</sup> The application of these currents poses the possibility to selectively switch different free magnetic layers.

## II. METHODS

In the presented work we implemented the STT using an additional Slonczewski contribution<sup>4</sup> to the Landau-Lifshitz-Gilbert (LLG) equation.

$$\begin{aligned} \frac{d\hat{m}}{dt} = & -\frac{|\gamma|}{(1+\alpha^2)} [\hat{m} \times \vec{H}_{eff}] \\ & -\frac{\alpha|\gamma|}{(1+\alpha^2)} [\hat{m} \times (\hat{m} \times \hat{H}_{eff})] \\ & +J_e \frac{|\gamma|}{(1+\alpha^2)M_S} \eta(\theta) [\hat{m} \times (\hat{m} \times \hat{p})] \\ & -J_e \frac{\alpha|\gamma|}{(1+\alpha^2)M_S} \eta(\theta) [\hat{m} \times \hat{p}] \end{aligned} \quad (1)$$

with<sup>11</sup>

$$\eta(\theta) = \frac{4\hbar}{\mu_0|e|d} \cdot \frac{\varepsilon^{\frac{3}{2}}}{3(1+\varepsilon)^3 - 16\varepsilon^{\frac{3}{2}} + (1+\varepsilon)^3 \cos(\theta)}$$

<sup>a)</sup>Electronic mail: christoph.vogler@tuwien.ac.at.

in our finite element package FEMME.<sup>12</sup>  $\hat{m}$  is the magnetization of the free magnetic layer normalized by the saturation magnetization  $M_S$  and  $\vec{H}_{eff}$  is the effective magnetic field, which can be derived from the total energy of the free layer with volume  $V$ .

$$\vec{H}_{eff} = -\frac{1}{\mu_0 V} \frac{\partial E_{tot}}{\partial \hat{m}} \quad (2)$$

The unit vector  $\hat{p}$  gives the direction of the spin polarization and  $\cos(\theta) = \hat{m} \cdot \hat{p}$ . The electric current density  $J_e$  is constant for a direct current (DC) and  $\propto \cos(\omega t)$  for an AC. Furthermore,  $d$  is the thickness of the free layer,  $\gamma$  is the gyromagnetic ratio ( $|\gamma| = 2.213 \cdot 10^5$  m/As),  $\alpha$  is the damping parameter and  $\varepsilon$  ( $0 < \varepsilon < 1$ ) gives the degree of spin-polarization ( $e$  is the electron charge,  $\mu_0$  is the vacuum permeability and  $\hbar$  is the reduced Planck constant). Due to the fact that a realistic damping constant of  $\alpha = 0.012$  is used in all simulations, the last term in Eq. (1) is neglected, because it gives only a small contribution to the precessional motion of the magnetization around the effective field.

The switching behavior of two different full micromagnetic models is investigated. A small prism structure (model M1: 0.5 nm × 3 nm × 10 nm) with neglected shape anisotropy and a larger more realistic model with an elliptic area (model M2: 6 nm × 10 nm × 20 nm) without uniaxial anisotropy but with shape anisotropy are used. Although, due to its size, model M1 is not thermally stable, it is very instructive to use this simple model to demonstrate the switching dynamics of the magnetization when spin-polarized currents are applied. In the last part of this work, it is shown that model M2, which is thermally stable, shows the same dynamics. So the results of model M1 are similarly valid for real memory bits of appropriate size (model M2). All models have the exchange constant ( $A = 2.5 \cdot 10^{-11}$  J/m) and the same saturation magnetization ( $M_S = 1.71 \cdot 10^6$  A/m). Model M1 is located in the  $y$ - $z$ -plane with an easy axis  $10^\circ$  off the  $z$ -axis. The long axis of the particle is parallel to the easy

axis. Two different materials with the crystalline anisotropy constants  $K_{1,layer1} = 305 \text{ kJ/m}^3$  and  $K_{1,layer2} = 247 \text{ kJ/m}^3$  are investigated. The applied current flows in the  $x$ -direction. It is spin-polarized in the  $z$ -direction with 30% more spin-up electrons than spin-down electrons ( $\varepsilon = 0.3$ ). The current profile is a 20.2 ns pulse with a current rise time and a current decay time of 0.1 ns respectively. The magnetization configuration in all presented simulations starts from a homogeneous magnetization parallel to the easy axis (P). The applied positive currents tend to switch the magnetization, therefore, into an anti-parallel state (AP).

### III. ORIGIN OF RESONANT SWITCHING

Prior to looking at the effect of a spin-polarized AC acting on the precessional motion of the magnetization it is important to understand the interplay of the damping and the amplifying torques when a spin-polarized DC is applied to a small model that behaves like a Stoner-Wolfarth particle such as model M1 and M2. In Fig. 1, two positions of the average magnetization are shown, at which  $M_{z,min}$  refers to the position where  $M_z$  is minimal during one precession period.  $M_{z,max}$  refers to the maximum  $z$ -component vice versa. According to Slonczewskis<sup>4</sup> formula, the STT depends on the sign of the current and the transversal part of the incoming spins relative to the direction of the magnetization. Furthermore, these two parts determine completely the direction of the resulting torque. The latter can be calculated from the angle between the  $z$ -axis and the magnetization vector.

If a DC polarized in the  $z$ -direction is used to exert a torque on the magnetization the sign of the current always remains the same. So only the angle between the  $z$ -axis and  $\vec{M}$  changes during a precessional rotation. This angle is larger

at  $M_{z,min}$  than at  $M_{z,max}$  as it can be seen in Figs. 1(a) and 1(b). Hence, the absolute value of the STT is larger when the magnetization passes  $M_{z,min}$ , as it is shown by means of a large arrow ( $d\vec{M}_{STT}/dt$ ) in Fig. 1(a). After calculating the exact direction of the STT it turns out that the torque acts as a strong amplifying force when the magnetization reaches its  $z$ -minimum and that it acts as a weak damping force when it reaches its  $z$ -maximum. If the amplitude of the DC overcomes a critical value the magnetization will switch in the negative  $z$ -direction.

The situation is different if an AC is applied to the magnetization, because the current now changes its sign. The sign of the STT depends on whether the positive half-wave or the negative half-wave of the current acts on the magnitude. If the maximum of the positive AC half-wave acts on the magnetization at  $M_{z,min}$  the result is the same as for a DC with the same amplitude. A large amplifying STT acts on the magnitude due to a large angle between the  $z$ -axis and  $\vec{M}$  [see Fig. 1(c)]. If the frequency of the AC matches the precessional frequency of the magnetization the minimum of the negative AC half-wave coincides with  $M_{z,max}$ . Due to the changed sign of the current the STT also acts as an amplifying force at this position [see Fig. 1(d)]. At  $M_{z,max}$  the torque is smaller than at  $M_{z,min}$ , because the angle between the  $z$ -axis and the magnetization is smaller. On the basis of this schematic representation it is clear that the AC frequency has to be applied in phase with respect to the magnetization. This is the essential key to achieve an optimal amplification.

In the presented simulations, a superimposition of a spin-polarized DC and a spin-polarized AC are used to prove this mechanism. Moreover, phase adapted spin-polarized currents are applied to demonstrate the possibility of selectively addressing thin ferromagnetic structures with different eigenfrequencies.

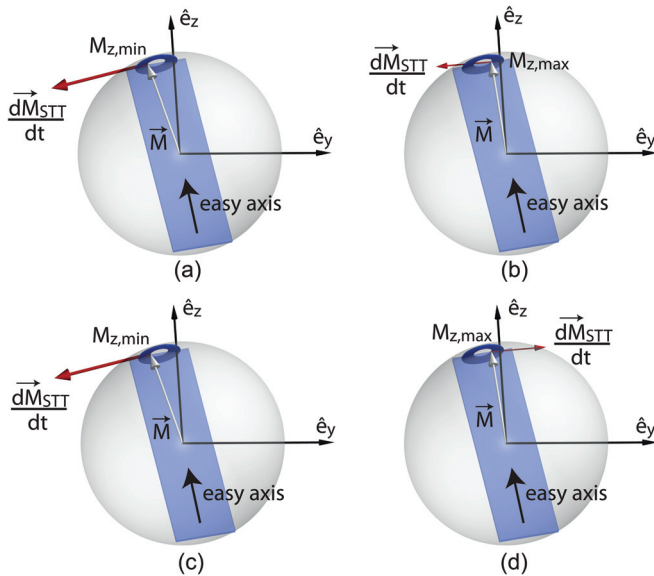


FIG. 1. (Color online) Effect of spin-polarized currents acting on the precessional motion of the magnetization. Model M1 is located in the  $y$ - $z$ -plane with an easy axis  $10^\circ$  off the  $z$ -axis. A DC is acting on the magnetization (a) at its minimum  $z$ -position and (b) at its maximum  $z$ -position. (c) The positive half-wave of an AC is acting on the magnetization at its minimum  $z$ -position. (d) The negative half-wave of an AC is acting on the magnetization at its maximum  $z$ -position. The arrows ( $d\vec{M}_{STT}/dt$ ) show the resulting STT.

## IV. RESULTS AND DISCUSSION

### A. Model M1

To demonstrate the frequency dependence of the critical switching DC density phase diagrams of two M1 models with different anisotropy constants  $K_1$  ( $247 \text{ kJ/m}^3$  and  $305 \text{ kJ/m}^3$ ) are shown in Fig. 2. The DC density varies between  $200 \text{ GA/m}^2$  and  $500 \text{ GA/m}^2$  and the AC frequency is changed between 0 GHz and 15 GHz. According to the experimental setup of Florez *et al.*<sup>9,10</sup> a fixed AC density of comparable magnitude ( $200 \text{ GA/m}^2$ ) is used in all phase points. Averaging the  $z$ -component of the normalized magnetization over the last 5 ns of the simulation time leads to the color code of the phase diagram. In the white areas the magnetization remains in its initial parallel state (P). In the black areas, the magnetization completely switches in the AP state. In order to be able to distinguish between the two different materials the results for the softer magnetic one is presented transparent. A very sharp resonance effect is shown in Fig. 2. Also the boundary between the final P and AP states is very sharp. In a narrow frequency area the critical switching DC density can be reduced significantly. The frequency peaks ( $f_{R1} = 9.9 \text{ GHz}$  and  $f_{R2} = 8.0 \text{ GHz}$ ) of the materials with different values of  $K_1$  can thus easily be

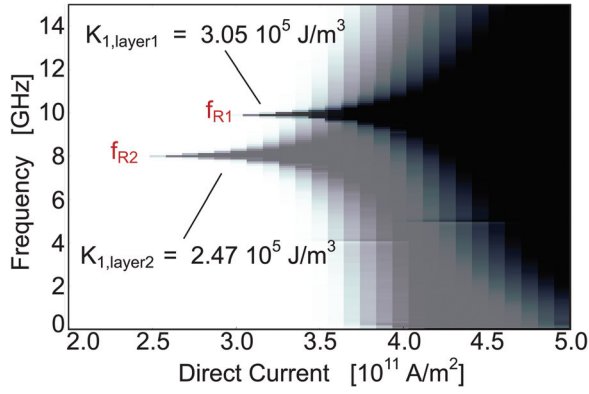


FIG. 2. (Color online) Phase diagram of two M1 models with different anisotropy constants ( $K_{1,layer1} = 305 \text{ kJ/m}^3$  and  $K_{1,layer2} = 247 \text{ kJ/m}^3$ ). The white areas show phase points where the  $z$ -component of the normalized magnetization is not switched out of its initial P state. In the dark points ( $M_z/M_s$ ) switched in the AP state.

distinguished. With a writing current consisting of an AC with a frequency of 9.9 GHz and a DC density of 310 GA/m<sup>2</sup> only the magnetic harder layer ( $K_{1,layer1} = 305 \text{ kJ/m}^3$ ) will be addressed and selectively switched. On the other hand a writing current with  $f_{AC} = 8.0 \text{ GHz}$  and DC = 270 GA/m<sup>2</sup> will only switch the softer magnetic layer ( $K_{1,layer2} = 247 \text{ kJ/m}^3$ ). The choice of the AC density of course influences the resonance effect. But a smaller AC density only lowers the absolute and not the relative resonance effect. This means that the lower the AC density gets the more the critical switching DC density increases at any value of  $f_{AC}$ , however the resonance peak still remains at the same position.

Figure 2 also reveals a restriction in the amount of possible layers, which can be selectively switched in one stack. The critical switching DC density decreases with smaller  $K_1$ . As a consequence the peak with the highest resonance frequency disappears behind the switched phase points of a material with too small  $K_1$ .

A closer look at the resonant phase point with  $K_{1,layer1} = 305 \text{ kJ/m}^3$ ,  $f_{AC} = 9.9 \text{ GHz}$  and DC = 300 GA/m<sup>2</sup> proves the above described mechanism as shown in Fig. 3. For  $f_{AC} = 9.9 \text{ GHz}$  the AC frequency matches the eigenfrequency of the magnetic harder layer best. The motion of the magnetization is in phase with the AC, which allows one to transfer a maximum of amplifying STT. The proposed mechanism can only be understood exactly if one takes care of the fact that a ferromagnetic layer has no definite eigenfrequency. The precessional frequency depends on the opening angle of the precessional motion of the magnetization and on the easy axis. Based on the analytical solution of Scholz *et al.*<sup>13</sup> we studied the precessional frequencies of various models, which differ in their dimensions and in their material constants. As long as the magnetization remains quasi homogeneous, we generally found that the precessional frequency follows a cosine function of the opening angle:

$$f(\alpha) = f_0 \cos(\alpha) \quad (3)$$

For the simple case of a model without shape anisotropy  $f_0$  can easily be calculated with  $f_0 = (\gamma K_1 / \mu_0 M_S \pi)$ . At the

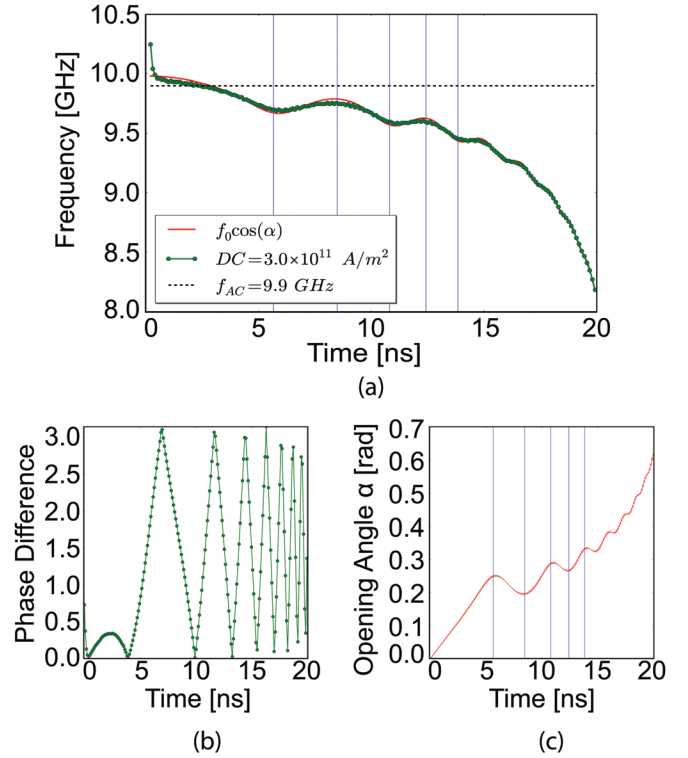


FIG. 3. (Color online) Phase point of Fig. 2 with  $K_{1,layer1} = 305 \text{ kJ/m}^3$ , an AC frequency of  $f_{AC} = 9.9 \text{ GHz}$  and a DC density of 300 GA/m<sup>2</sup>. (a) Simulated frequency evolution of the precessional motion of the magnetization and the calculated curve from its opening angle (c)  $f_0 \cos(\alpha)$ . (b) Phase difference between the AC frequency and the motion of magnetization. The vertical lines show the times when the phase shift passes  $(\pi/2)$ .

beginning of the simulation, where the magnetization is still almost homogeneous to the easy axis, the precessional frequency ( $f_{0,layer1} = 9.98 \text{ GHz}$ ) is marginal larger than the applied AC frequency ( $f_{AC} = 9.9 \text{ GHz}$ ), which can be seen in Fig. 3(a). Due to this mismatch of frequencies the phase difference is hence increasing as shown in Fig. 3(b). Because of the amplifying STT at low phase differences the opening angle increases [see Fig. 3(c)]. Thus the precessional frequency decreases. At approximately 2.5 ns the two frequency lines cross each other and from that time on the  $f_{AC}$  is always larger than the precessional frequency. As a consequence the phase difference decreases again. This mechanism permits the phase difference to remain clearly below  $(\pi/2)$  for more than 5 ns. Thus, the critical switching DC density can be decreased in a small frequency area marginal below  $f_{0,layer1}$ .

If a slightly lower AC frequency of  $f_{AC} = 9.8 \text{ GHz}$  is used to trigger the magnetization the phase difference increases too fast. Therefore, the amplifying STT is too weak to increase the opening angle as much as necessary to lower the system frequency below 9.8 GHz. The frequency lines do not cross each other and so the phase difference increases. If the AC frequency and the precessional motion are in anti-phase the AC causes an optimal damping STT. The magnetization reacts and increases the precessional frequency rapidly for a few periods to decrease the phase difference again. This frequency pulling effect was also described by Florez *et al.*<sup>9,10</sup> In our simulations, it occurs only in the

non-resonant regimes and is not important for the main resonance effect.

## B. Optimization

With a constant AC frequency it is not possible to lower the critical switching DC density further. However, if the AC frequency is triggered by the precessional frequency of the magnetization it is possible to keep them almost in-phase for the whole switching time. Hence the simulation shows that a DC density of  $260 \text{ GA/m}^2$  is able to completely switch the magnetization for the layer with  $K_{1,layer1} = 305 \text{ kJ/m}^3$ . Compared with the phase diagram in Fig. 2 it is a further reduction of the minimal critical switching DC density of about 20%.

## C. Model M2

A phase diagram of the model M2, which is thermal stable with an energy barrier of  $83 k_B T_{300}$  (Ref. 14), shows the same shape as seen for the models M1. There exists a narrow resonance peak and a sharp boundary between P and AP states. But this is only valid as long as the average magnetization of the layer remains almost homogeneous. For models with larger lateral dimensions the path of the magnetization does not follow a traditional precession any longer and cannot be triggered efficiently with an AC frequency. So the resonance effect disappears.

## V. CONCLUSION

In conclusion, we demonstrate that the essential key for optimal amplifying STT is to keep the phase difference between the precessional motion of the mean magnetization and the AC frequency small. As long as they act in-phase a combination of an AC and a DC can decrease the critical switching DC density of this superposition. With a constant

AC frequency the phase difference can only be kept small for longer times in a very narrow range marginal below the eigenfrequency  $f_0$ . Thus, the resonance effect is very sharp. The eigenfrequency depends on the material constants and on the shape of the used layers, so it is possible to address them selectively and reliably. This is valid for realistic memory bits of appropriate size. A further decrease of the critical switching DC density can be accomplished by using a dynamic AC frequency, which follows the precessional frequency of the magnetization.

## ACKNOWLEDGMENTS

The authors would like to thank the WWTF Project MA09-029 and FWF Project SFB-ViCoM, F4112-N13 for the financial support.

- <sup>1</sup>J. Åkerman, *Science* **308**, 508 (2005).
- <sup>2</sup>J. C. Slonczewski, *Phys. Rev. B* **39**, 6995 (1989).
- <sup>3</sup>L. Berger, *Phys. Rev. B* **54**, 9353 (1996).
- <sup>4</sup>J. C. Slonczewski, *J. Magn. Magn. Mater.* **159**, L1 (1996).
- <sup>5</sup>M. Tsoi, A. G. M. Jansen, J. Bass, W.-C. Chiang, M. Seck, V. Tsoi, and P. Wyder, *Phys. Rev. Lett.* **80**, 4281 (1998).
- <sup>6</sup>J. A. Katine, F. J. Albert, R. A. Buhrman, E. B. Myers, and D. C. Ralph, *Phys. Rev. Lett.* **84**, 3149 (2000).
- <sup>7</sup>J. Miltat, G. Albuquerque, A. Thiaville, and C. Vouille, *J. Appl. Phys.* **89**, 6982 (2001).
- <sup>8</sup>E. B. Myers, D. C. Ralph, J. A. Katine, F. J. Albert, and R. A. Buhrman, *J. Appl. Phys.* **87**, 5502 (2000).
- <sup>9</sup>S. H. Florez, J. A. Katine, M. Carey, L. Folks, and B. D. Terris, *J. Appl. Phys.* **103**, 07A708 (2008).
- <sup>10</sup>S. H. Florez, J. A. Katine, M. Carey, L. Folks, O. Ozatay, and B. D. Terris, *Phys. Rev. B* **78**, 184403 (2008).
- <sup>11</sup>R. Bonin, G. Bertotti, I. D. Mayergoyz and C. Serpico, *J. Appl. Phys.* **99**, 08G508 (2006).
- <sup>12</sup>D. Suess, V. Tsiantos, T. Schrefl, J. Fidler, W. Scholz, H. Forster, R. Dittrich, and J. J. Miles, *J. Magn. Magn. Mater.* **248**, 298 (2002).
- <sup>13</sup>W. Scholz, T. M. Crawford, G. J. Parker, T. W. Clinton, T. Ambrose, S. Kaka, and S. Batra, *IEEE Trans. Magn.* **44**, 3134 (2008).
- <sup>14</sup>R. Dittrich, T. Schrefl, D. Suess, W. Scholz, H. Forster, and J. Fidler, *J. Magn. Magn. Mater.* **250**, 12 (2002).

Journal of Applied Physics is copyrighted by the American Institute of Physics (AIP). Redistribution of journal material is subject to the AIP online journal license and/or AIP copyright. For more information, see <http://ojps.aip.org/japo/japcr/jsp>